ALTEX preprint
published June 23, 2020
doi:10.14573/altex.2003182

Research Article

Examination of Microcystin Neurotoxicity Using Central and Peripheral Human Neurons

Stefanie Klima[1,2], Ilinca Suciu[1,5], Lisa Hoelting[1], Simon Gutbier[1] Tanja Waldmann[1] ,Daniel Dietrich[2,3], Marcel Leist[1,4]

[1]In vitro Toxicology and Biomedicine, Dept inaugurated by the Doerenkamp-Zbinden Foundation, University of Konstanz, Konstanz, Germany; [2]Cooperative doctorate college InViTe, University of Konstanz, Konstanz, Germany; [3]Human and Environmental Toxicology, University of Konstanz, Konstanz, Germany; [4]CAAT-Europe, University of Konstanz, Konstanz, Germany; [5]Konstanz Research School Chemical Biology (KoRS-CB), University of Konstanz, Konstanz, Germany

Abstract

Microcystins (MC) are a group of cyanobacterial toxins that comprises MC-LF and other cyclic heptapeptides, best known as potent hepatotoxicants. Cell culture and epidemiological studies suggest that MC might also affect the nervous system, when there is systemic exposure e.g. via drinking water or food. We asked whether in vitro studies with human neurons could provide estimates on the neurotoxicity hazard of MC-LF. First, we used LUHMES neurons, a well-established test system for neurotoxicants and neuropathological processes. These central nervous system cells expressed OATP1A2, a presumed carrier of MC-LF, and we observed selective neurite toxicity in the µM range (EC20 = 3.3 µM ≈ 3.3 µg/ml). Toxicity paralleled transcriptome changes pointed towards attenuated cell maintenance and biosynthetic processes. Prolonged exposure for up to four days did not increase toxicity. As a second model, we used human dorsal root ganglia-like neurons. These peripheral nervous system cells represent parts of the nervous system not protected by the blood brain barrier in humans. Toxicity was observed in a similar concentration range (EC20 = 7.4 µM). We conclude that MC-LF poses a potential neurotoxic hazard in humans. The adverse effect concentrations observed here were orders of magnitude higher than those presumed to be encountered after normal nutritional or environmental exposure. However, the low µM concentrations found to be toxic are close to levels that may be reached after very excessive algae supplement intake.

1 Introduction

While microcystins (MCs) are widely known for their acute hepatotoxicity (Carmichael, 1992; Nishiwaki-Matsushima et al., 1992), their potentially adverse effects on other target organs, such as the nervous system, are less clear. MCs are small cyclic heptapeptides comprised of 5 D- and 2 L-amino acids (cyclo-d-Ala[1]-X[2]-d-MeAsp[3]-Z[4]-Adda[5]-d-Glu[6]-Mdha[7]). Structural variation of side-chains has been encountered in all seven positions, but the most variable amino acids (X and Z) are the L-amino acids in positions 2 and 4 (Botes D.P., 1984; Daneshian et al., 2013). These variable L-amino acid residues are used for naming of the MC congeners, of which more than 248 different congeners are known to date (Altaner et al., 2019; Spoof and Catherine, 2016). For example in MC-LF these amino acids are L-leucine (L) and L-phenylalanine (F). A number of ubiquitously present cyanobacteria genera, e.g. *Microcystis*, *Planktothrix*, *Anabaena*, *Dolichospermum*, have been demonstrated to produce MC (Svirčev et al., 2019).

The main exposure route for humans is drinking water, albeit excessive exposure can occur when cyanobacterial supplements are voluntarily consumed (Heussner et al., 2012; Dietrich and Hoeger, 2005). The World Health Organization (WHO) suggested a safe value of 1 µg/l (1 nM) for MC-LR into their guidance on cyanobacteria in drinking[1]. Based on the latter, the tolerable daily intake (TDI) for a human was calculated to be 0.04 µg $MC\text{-}LR_{equivalents}$/kg body weight/day (≈ 40 pmol/kg body

Received March 18, 2020; Accepted June 9, 2020;
Epub June 23, 2020;

ALTEX 37(#), ###-###. doi:10.14573/altex.2003182

Correspondence: Marcel Leist, PhD
In vitro Toxicology and Biomedicine,
Dept inaugurated by the Doerenkamp-Zbinden Foundation
University of Konstanz
Universitaetsstr. 10
78457 Konstanz, Germany
(marcel.leist@uni-konstanz.de)

[1] https://www.who.int/water_sanitation_health/dwq/GDWQ2004web.pdf?bcsi_

weight/day). In addition to the well-established hepatotoxicity, also renal- and neurotoxicity have been reported based on in vivo and in vitro experiments in rodents, fish and birds (Fischer and Dietrich, 2000; Feurstein et al., 2009, 2011; Hu et al., 2016; Herrera et al., 2018; Hinojosa et al., 2019).

There are several reported human exposures to MCs with an adverse outcome. In Caruaru (Jochimsen et al., 1998; Pouria et al., 1998), patients at a haemodialysis clinic were accidentally exposed via dialysis water with an estimated MC concentration of 19.5 µg/l (20 nM) (Azevedo et al., 2002). The symptoms reported in the patients ranged from early visual disturbances to muscle weakness and nausea. Of the 126 - 131 patients, hundred developed acute liver toxicity and between 52 and 60 of them died within 10 months (Azevedo et al., 2002; Pouria et al., 1998).

At lake Chaohu, China, fishermen were chronically exposed to MCs by drinking water and food. Concentrations of MC were 3.28 µg/l, which corresponds to 3.3 nM MC-$LR_{equivalents}$ in drinking water. The muscle of contaminated aquatic animals showed MC concentrations of 43 ng/g dry weight (DW) (43 pmol MC-$LR_{equivalent}$/g DW) which led to blood concentrations in fishermen ranging from 0.045 to 1.832 ng/ml (0.045 to 1.84 pM) (Chen et al., 2009). The blood samples showed increased levels of liver enzymes like alanine aminotransferase.

In the three gorges reservoir region of China, more than 1000 children were chronically exposed to MC. They showed elevated liver enzyme levels of alanine aminotransferase, compared to non-exposed children (Li et al., 2011). The average drinking water concentration of MC was 2.6 µg/l (2.6 nM), the mean concentration in fish was 0.22 µg/g DW (221.1 nmol/g DW).

MCs need to be actively transported into cells by organic anion transporting polypeptides (OATPs). Cells of the blood brain barrier as well as neurons express OATP1A2 (Hagenbuch and Meier, 2003; Bronger et al., 2005). This suggests that MCs can cross the blood brain barrier, as OATP1A2 was demonstrated to transport MC-LR (Fischer et al., 2005). The best-documented mode of action of MC in mammalian cells (hepatocytes) is the inhibition of serine/threonine-specific protein phosphatase 1, 2A and 5 (MacKintosh et al., 1990; Buratti et al., 2017; Valério et al., 2016; Chen and Xie, 2016; Altaner et al., 2020). This results in a hyperphosphorylation of several protein kinase targets, which eventually leads to a widespread dysregulation of cellular processes (Yoshizawa et al., 1990; MacKintosh et al., 1990; Hinojosa et al., 2019).

As epidemiological and animal data from rodents, fish and birds suggest that MCs may not only induce hepatotoxicity, but also neurotoxicity, we explored the MC toxicity to human neurons. We used LUHMES cells, as representatives of central human neurons (Lotharius et al., 2005; Scholz et al., 2011). These cells have a normal karyotype (Gutbier et al., 2018) and typical neuronal structure and electrophysiology (Scholz et al., 2011). They have been widely used as alternatives to animal testing and in neuropathology studies (Witt et al., 2017; Lohren et al., 2015; Delp et al., 2019; Singh et al., 2018; Scholz et al., 2018; Delp et al., 2018; Tong et al., 2018; Höllerhage et al., 2017; Devos et al., 2014; Skirzewski et al., 2018). As second, complementary test system, we used human peripheral neurons. These were generated from pluripotent stem cells (Hoelting et al., 2016). They were established as a screening system for peripheral neurotoxicants (Delp et al., 2018). These models were used as *in vitro* approach to identify neurotoxic MC concentrations in order to compare them to serum concentrations reported in humans after exposure.

2 Materials and methods[2]

Material

Cisplatin, valinomycin, tubacin, microcystin-LF, microcystin-LR, PLO, fibronectin, glutamine, tetracycline, cAMP, apotransferrin, glucose, insulin, putrescine, selenium, progesterone and calcein-AM were purchased from Sigma, USA. AdvDMEM/F12, knockout serum replacement, DMEM/F12, N2 supplement, Glutamax, NEAA, ß-mercaptoethanol, Triton-X-100, PBS, H-33342, FBS, Trizol, Flou-4 Direct™ Calcium Assay Kit were purchased from ThermoFisher Scientific, USA. FGF2, GDNF, noggin, BDNF and NGF were purchased from R&D systems, USA. Dorsomorphin, SB-431642 and SU5402 were purchased from Torcis, UK. Chir99021 was purchased from Axon Medchem, USA, DAPT was purchased from Merck Millipore, USA. Matrigel was purchased from Corning, USA, iScript and SsoFast™ EvaGreen® Supermix were purchased from BioRad, USA. Pacific ciguatoxin (pCTX) isolated from a moray eel, was provided by the laboratory of Richard Lewis, University of Queensland, Brisbane, Australia. Chemical structures were drawn with ChemDraw (Version 16.0) from PerkinElmer.

LUHMES culture

LUHMES were used for modeling central human neurons and cultured as described earlier (Krug et al., 2013; Lotharius et al., 2005; Scholz et al., 2011). Briefly, cells were cultured on PLO/fibronectin (50 µg/ml poly-L-ornithine (PLO) and 1 µg/ml fibronectin) coated flasks and plates. Cells were maintained in proliferation medium (AdvDMEM/F12 supplemented with 2 mM glutamine, 1x N2 supplement and 40 ng/ml fibroblast growth factor-2 (FGF2)). Differentiation was started by seeding cells at a density of 100,000 cells/cm^2 in proliferation medium and changing the medium after 24 h to differentiation medium (AdvDMEM/F12 supplemented with 2 mM glutamine, 1x N2 supplement, 2.25 µM tetracycline, 1 mM dibutyryl 3',5'-cyclic adenosine monophosphate (cAMP) and 2 ng/ml recombinant human glial cell derived neurotrophic factor (GDNF)). Medium change was performed every 48 h after the differentiation was started.

---

[2] *Abbreviations:* DEG, differentially expressed genes; DMSO, dimethylsulfoxide; DoD, day of differentiation; DW, dry weight; MC, microcystin; OATP, organic anion transporting polypeptides; oGOs, overrepresentation of gene ontologies; PCA, principal component analysis; pCTX, pacific ciguatoxin

ALTEX preprint
published June 23, 2020
doi:10.14573/altex.2003182

Peripheral neurons

The stem cell line (WA09 line) was obtained from WiCell (Madison, WI, USA). The pluripotent stem cells were differentiated into immature dorsal root ganglia like neurons exactly according to the protocol of Hoelting et al. (Hoelting et al., 2016). Briefly, differentiation was started on day of differentiation (DoD) 0' by adding neural differentiation medium (KSR-S; knockout DMEM with 15% serum replacement, 1 x Glutamax, 1 x non-essential amino acids, and 50 µM ß-mercaptoethanol) and six small molecule pathway inhibitors (35 ng/ml noggin, 600 nM dorsomorphin, 10 µM SB-431642, 1.5 µM CHIR99021, 1.5 µM SU5402 and 5 µM DAPT). Starting from DoD4', medium was gradually replaced by N2-S medium (DMEM/F12, with 2 mM Glutamax, 0.1 mg/ml apotransferrin, 1.55 mg/ml glucose, 25 mg/ml insulin, 100 mM putrescine, 30 nM selenium, and 20 nM progesterone). After eight days of differentiation, the neuronal precursors were cryopreserved. After thawing, cells were seeded at a density of 100,000 cells/cm^2 in 25% KSR-S and 75% N2-S supplemented with 1.5 µM CHIR99021, 1.5 µM SU5402 and 5 µM DAPT. On DoD1 and DoD2, 50% of the medium was changed. From DoD3 on cells received N2-S medium, supplemented with 10 ng/ml BNDF, 10 ng/ml GNDF and 25 ng/ml NGF for further differentiation and maturation, with medium changes every other day.

Ca^{2+} signaling

Peripheral neurons were seeded at a density of 100,000 cells/cm^2 and cultured according to Hoelting et al. (Hoelting et al., 2016). After 23 days of differentiation, the cells were loaded with Fluo4 AM-Calcium Assay Kit and Hoechst-33342 (H-33342) for 20 min at 37°C. Changes in the free intracellular Ca^{2+} concentration were monitored with VTI HCS microscope (Cellomics, USA) containing an incubation chamber providing an atmosphere with 5% CO_2 and 37°C. Substances (Hank's balanced salt solution, 0.3% dimethylsulfoxide (DMSO), 2.5 µM MC-LF, 30 mM KCl, 15 nM pCTX) were administered by an automated pipettor 10 s after the first image was taken. Images were taken as fast as possible for 45 s (approx. one image/second) and exported as .avi files. The files were analysed in CaFFEE software (Karreman et al., 2020).

Viability testing

LUHMES and peripheral neurons were seeded at a density of 100,000 cells/cm^2, cultured and treated as indicated in the respective figure. One hour prior to analysis cells were stained with staining mix (1 µg/ml H-33342 and 1 µM calcein-AM), incubated one hour at 37°C and image acquisition was performed automatically with ArrayScan VTI HCS microscope (Cellomics, USA). Analysis of the pictures was performed as described earlier (Stiegler et al., 2011). Briefly, the neuronal area was identified by calcein stain and the somatic area was subtracted, which resulted in definition of neurite area. The viability was obtained from the same images. Cells with a double stain for H-33342 and calcein were counted as alive, whereas cells only positive for H-33342 were classified as dead.

Immunofluorescence and microscopy

Cells were grown on coated 96 well plates and fixed with 4% paraformaldehyde on day 6 (LUHMES) or DoD7 (peripheral neurons). Following permeabilisation in 0.3% Triton X-100, they were blocked 1 h in PBS containing 5% fetal bovine serum and 0.1% Triton X-100. Primary antibodies (Tuj1 (BioLegend Cat. No. 801202) 1:1000, OATP1A2 (Sigma-Aldrich Cat. No. SAB4502814) 1:100, Peripherin (Santa Cruz Cat. No. sc-7604) 1:200) were added for 1 h at room temperature. After washing, secondary antibodies and H-33342 were incubated for 30 min. Images were taken at a Zeiss Axio Observer with ZEN 2 pro blue edition software and further processed with ImageJ (Version 1.52p).

RNA extraction, cDNA synthesis and real-time qPCR

Total RNA was extracted using TRIzol, according to the manufacture's protocol. Total RNA (1 µg) was reverse transcribed with iScript. Quantification of cDNA was performed using the SsoFast^{TM} EvaGreen® Supermix. The threshold cycle (C_T) was determined for each sample, using the CFX data analysis software (Bio-Rad, USA). As reference gene RPL13A was used (forward: GGTATGCTGCCCCACAAAACC reverse: CTGTCACTGCCTGGTACTTCCA), mRNA levels of OATP1A2 (forward: TCCTGTGTGTGGAAACAATG reverse: AGCATCAAGGAACAGTCAGG) and OATP3A1 (forward: CTGGGCTCTTTCTGTACCAA reverse: GTGGAAACCCAAACATCAAG) were compared to reference gene using the ΔΔ method (Livak and Schmittgen, 2001).

Transcriptome data generation and analysis

For the sample preparation, the medium was removed from each well and cells were immediately lysed in 25 µl of 1x Biospyder lysis buffer. Storage was done at -80ºC until samples were shipped to Bioclavis (BioSpyder Tech.) on dry ice. The assay used for the transcriptomics data is TempO-Seq, a targeted RNA-sequencing method developed by BioSpyder Technologies, Inc, described in detail in (House et al., 2017).

For the transcriptomics data analysis, the R package DESeq2 (v1.24.0) was employed (Love et al., 2014). The DESeq2 object was constructed from raw counts and its size factors were coerced to total sample counts per million (CPM). The analysis of differential gene expression in the treatment group (against the DMSO control group) was done with the Wald test. In order for a gene to be considered significantly deregulated, the threshold of Benjamini-Hochberg adjusted p-values ≤ 0.05 had to be satisfied. Overrepresentation analysis was based on Fisher's F-test as implemented in G-profiler software (Raudvere et al., 2019). Principal component analysis (PCA) was generated with the online tool ClustVis (Metsalu and Vilo, 2015).

Statistics

Experiments were performed at least on two (usually on three) cell preparations, with several (≥3) technical replicates for each cell batch. For statistical analysis GraphPad Prism 5 software (Version 5.03) was used. Data were evaluated by ANOVA with post-hoc testing (Dunnett's), or by t-test (two groups) as appropriate. P-values <0.05 were regarded as statistically significant. For curve fitting a four-parameter fit with top constrains set to 100% was used in GraphPad Prism 5 software (Version 5.03).

3 Results and discussion

3.1 Neurotoxicity of MC-LF, assessed on LUHMES neurons

LUHMES neurons, differentiated for 4-6 days are not only fully post-mitotic (Scholz et al., 2011), but also show many features of central nervous system cells (Tong et al., 2018; Gutbier et al., 2018; Matelski et al., 2020; Weng et al., 2012, 2014). The cells were also found here to be positive for OATP1A2, a transporter that accepts microcystins (MCs) as substrate (Fig. 1A) (Fischer et al., 2005: Chen and Xie, 2016). When LUHMES cells were exposed to MC-LF (Fig. 1B) for 48 h, we observed a specific neurite degeneration at concentrations above about 2 µM (Fig. 1 C and D). The number of viable cells (= cell bodies) was not affected at concentrations as high as 5 µM (Fig. 1C). Follow-up experiments showed that 24 h exposure was not sufficient to trigger neurite damage (Fig. S1 A-C[3]). Exposure of 24 h, followed by a 24 h washout period led to the same toxicity as 48 h continuous exposure (Fig. S1D[3]). This suggests that toxic effects were all triggered during the first 24 h, but manifestation of toxicity (neurite breakdown) took one day more to develop. We tested whether even longer times would allow for more potent toxicant effects. However, exposure for 48 h, followed by a 48 h washout (4 days in total) did not lead to more potent effects of MC-LF (Fig. S1E[3]). To further investigate effect specificity, we also investigated MC-LR (Fig. S1F[3]), known to be a less potent toxicant (Feurstein et al., 2011). Indeed, no toxicity was observed here at concentrations up to 5 µM (Fig. S1G[3]). To test for potentially more subtle effects of MC on neurons, serveral other endpoints were considered. Tau phosphorylation and activation of MAP kinases (ErK) were examined by Western blotting, but no changes were observed at ≤ 5 µM MC-LF (data not shown). For this series of experiments, we concluded that MC-LF can trigger neurotoxicity at high concentrations (> 2 µM). Our data based on established and sensitive endpoints of neurite toxicity suggest that lower concentrations of MC-LF are inactive in the chosen experimental model of human neurons and with the exposure scenarios scrutinized here.

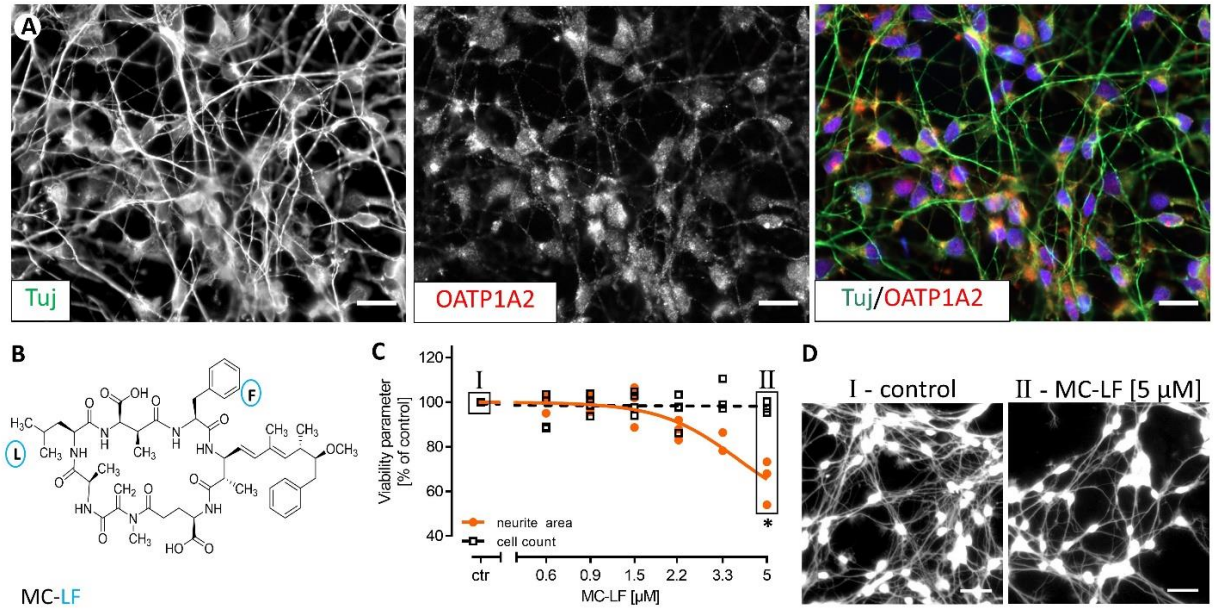

Fig. 1: Effect of MC-LF on LUHMES neurons

(A) LUHMES cells were differentiated on coverslips and fixed after six days. Double-immunofluorescence images were obtained for neurite structures (using an antibody against ß-III- tubulin, Tuj) and for OATP1A2. For maximum clarity the individual channels are shown in b/w, the composite image is shown with neurites in green and OATP1A2 in red. Scale bar is 20 µm. (B) Chemical structure of MC-LF. (C) Effect of MC-LF on neurite area (orange) and cell count (black), after 48 h treatment from d4 until d6. Data points are from three separate experiments, *p<0.05. (D) Exemplary pictures of calcein-stained cells treated with 5 µM MC-LF (II) or solvent (I), as described in C. Scale bar is 50 µm.

[3] doi:10.14573/altex.2003182s1

ALTEX preprint
published June 23, 2020
doi:10.14573/altex.2003182

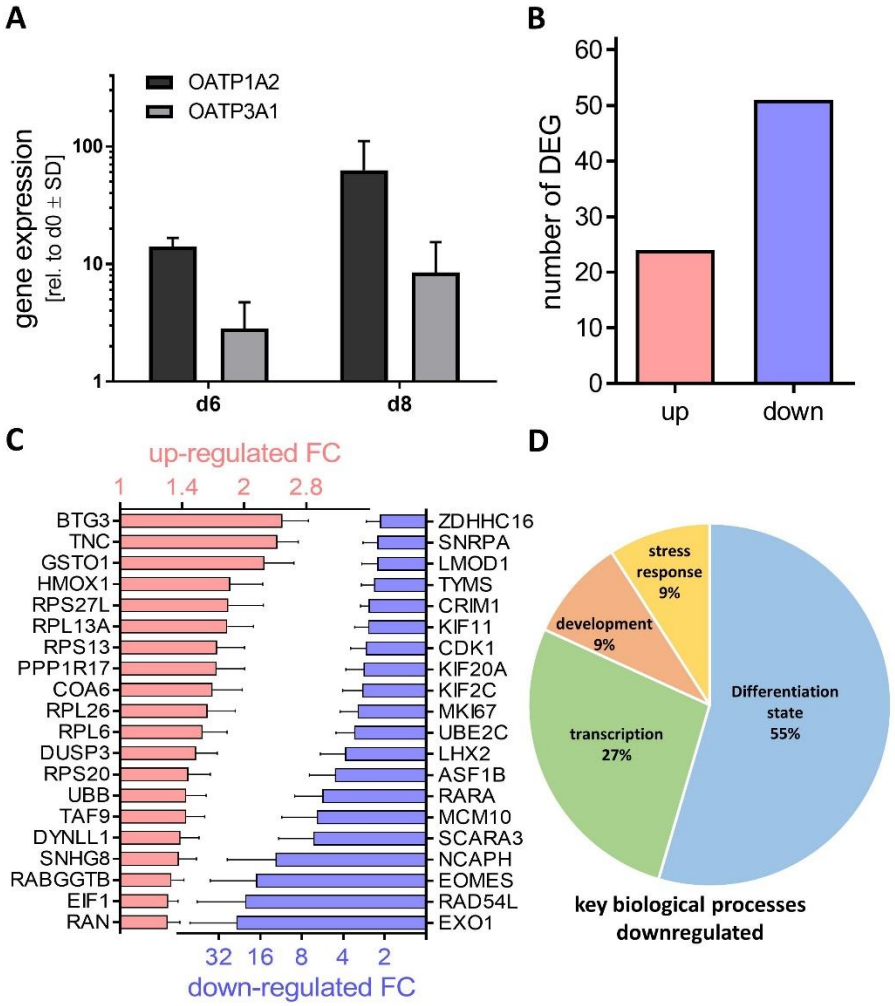

Fig. 2: Transcriptome analysis of MC-LF treated LUHMES
(A) OATP1A2 (black) and OATP3A1 (grey) expression levels of LUHMES on d6 and d8 relative to d0 determined with RT-qPCR. (n=2) (B) Samples were obtained at d6 from untreated LUHMES and LUHMES treated with 5 µM MC-LF for 48 h from d4 until d6 LUHMES, and RNA expression profiles were obtained. Number of differentially expressed genes (DEG) is shown for upregulations (red) and downregulations (blue) with an adjusted p-value ≤ 0.05. (C) Out of the DEGs in B the top 20 upregulated (red) and downregulated (blue) genes according to their fold change (FC) are shown. The error bars represent the standard deviation. (D) The gProfiler analysis tool was used to identify overrepresented GOs (oGOs) among the downregulated DEGs. These were then assigned to four different superordinate biological processes according to Waldmann et al. (Waldmann et al., 2014).

3.2 Transcriptome disturbances triggered by MC-LF

To broadly capture effects of MC on neurons, the transcriptional changes triggered by a 48 h treatment of 5 µM MC-LF were measured (Fig. S2A[3]). The PCA analysis clearly showed a separation between the MC treatment and the control (Fig. S2B[3]). The analysis identified 75 differentially expressed genes (DEGs) (Fig. 2B). The top downregulated DEGs were mainly related to differentiation and chromatin remodeling, such as EXO1, RAD54L or NCAPH and thus did not indicate specific pathways (Fig. 2C). The most upregulated DEGs include predominantly ribosomal genes like RRS27L, RPL13A, RPS13 and the anti proliferative factor BTG3. This pattern is consistent with a relatively unspecific cellular stress response. To get a better understanding of the DEGs, we performed a gene ontology overrepresentation analysis. The upregulated DEGs resulted in more than 20 overrepresented gene ontologies (oGO) (Fig. S2C[3]). Downregulated DEGs resulted in only eleven oGOs (Fig. S2D[3]). The gene PPP1R17 (protein phosphatase 1 regulatory subunit 17) is included in the oGOs “mRNA catabolic process”, “heterocycle catabolic process” (Fig. S2E[3]), “cellular nitrogen compound catabolic process” and “aromatic compound catabolic process”. Its gene product inhibits the phosphatase activities in protein phosphatase 1 (PP1) and protein phosphatase 2A (PP2A) complexes. The inhibition of PP1 and PP2A is also the best described direct mode of action of MCs (Altaner et al., 2020, MacKintosh et al., 1990, Chen and Xie, 2016, Buratti et al., 2017, Valério et al., 2016). It appears as if most of the downregulated DEGs are grouped into oGOs dealing with cell cycle (Fig. S2D[3]). But if investigated more precisely, the included genes in the respective oGOs are linked to cell cycle only very indirectly. Exemplarily, the DEGs included in the GO “mitotic nuclear division” are mainly genes related to (neuronal)

ALTEX preprint
published June 23, 2020
doi:10.14573/altex.2003182

differentiation status like EMX2, SNCA, and TCF4 (Fig. S2F[3]). To integrate the results of the downregulated DEGs and the GO analysis we assigned the oGOs to key biological processes according to Waldmann et al. (Waldmann et al., 2014) (Fig. 2D). Over 50% of the key biological processes of the downregulated oGOs can be assigned to genes involved in development and differentiation. The data of transcriptional changes after 48 h treatment with MC-LF point to an altered differentiation state of LUHMES, a typical generalized stress response in adult tissues (Desprez et al., 2019).

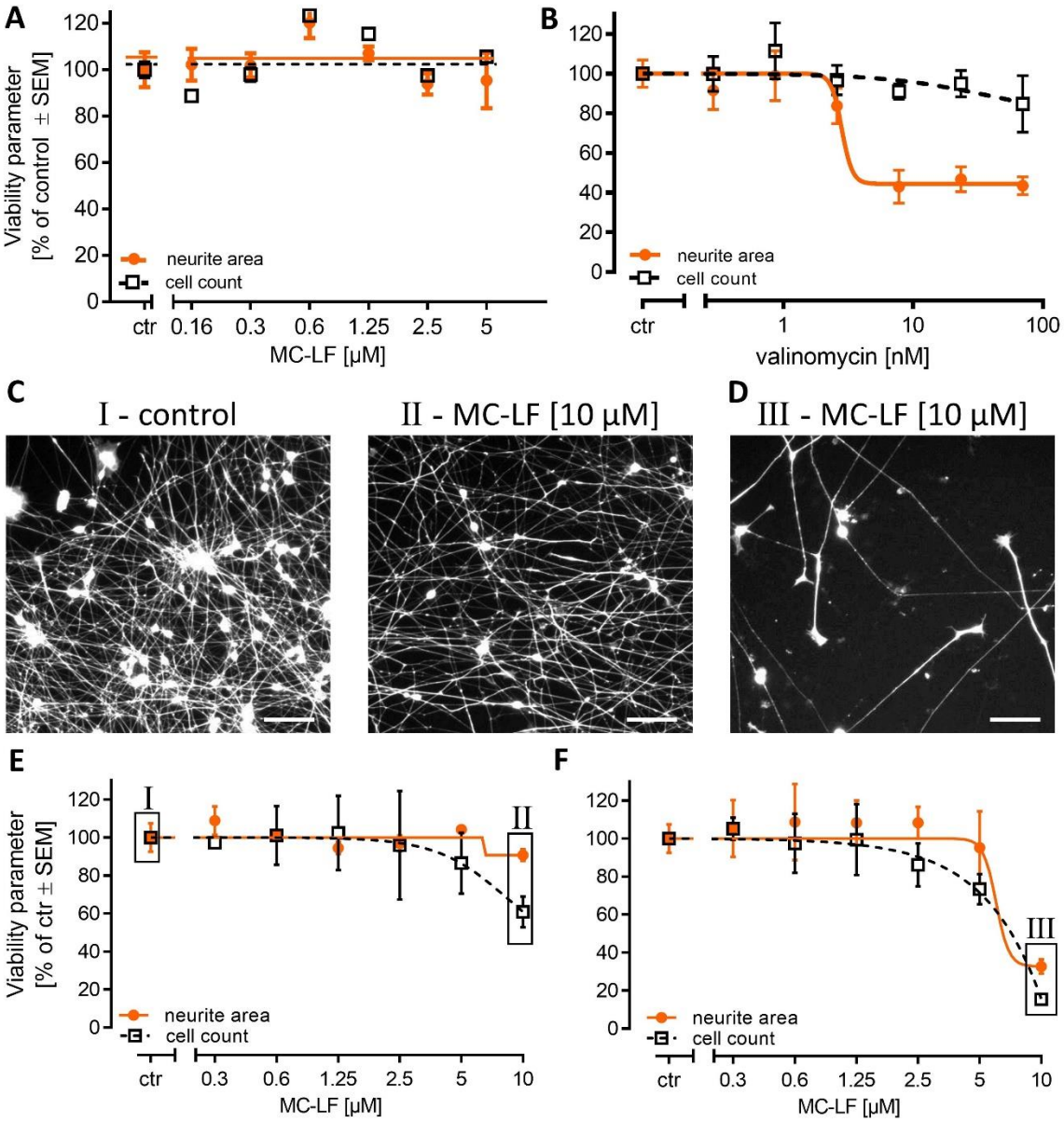

Fig. 3: Effect of MC-LF on peripheral neurons
Peripheral neurons were generated from human pluripotent stem cells according to an established protocol. After thawing, cells were immediately plated on 96-well plates and used for toxicity experiments. (A) Effect of MC-LF on neurite area (orange) and cell count (black) after a 24 h treatment from DoD0 until DoD1. Data are from three independent experiments. (B) Effect of the positive control valinomycin on neurite area (orange) and cell count (black) after treatment as in A. Data are from four independent experiments. (C and D) Exemplary pictures of calcein-stained cells treated with solvent (I) or 10 µM MC-LF for 48 h from DoD4 until DoD6 (II) or 10 µM MC-LF for 48 h from DoD4 until DoD6 followed by a 48 h washout period (III). Scale bar is 100 µm. (E) Effect of MC-LF on neurite area (orange) and cell count (black) after 48 h treatment from DoD4 until DoD6. Data are means ± SEM; n=3. (F) Effect of MC-LF on neurite area (orange) and cell count (black) after 48 h treatment (from DoD4 until DoD6) followed by a 48 h washout period. Data are means ± SEM; n=3.

3.3 Toxicity of MC-LF to peripheral human neurons

As a second neuronal test system we used human pluripotent stem cell derived peripheral neurons (Fig. S3A[3]). The cells can be generated in big batches and thawed as required for testing (Fig. S3B[3]). They provide a suitable test system for mechanistic studies (Hoelting et al., 2016) and screening approach (Delp et al., 2018). At DoD7 after thawing, the cells express the transporter OATP1A2, which is known to transport also MCs (Fig. S3C[3]). As peripheral neurons are not protected by the blood brain barrier, they could be more susceptible to neurotoxicants than neurons from the central nervous system. We used the PeriTox assay in which more than 100 substances have been tested (Hoelting et al., 2016; Delp et al., 2018), to investigate the effect of MC-LF on neurite outgrowth in peripheral neurons (Fig. 3A). As positive controls, valinomycin (Fig. 3B), a cyclic peptide, with L-amino acids, produced by *Streptomyces*, cisplatin, a chemotherapeutic drug, and tubacin, an HDAC inhibitor (Fig. S3D[3]), were used. Tubacin, as a specific HDAC6 inhibitor, catalyzes α-tubulin acetylation (Gao et al., 2007) and thereby interferes with neurite outgrowth. An often-observed side effect of chemotherapeutic drugs are peripheral neuropathies, which can be mimicked by cisplatin application. As no changes in viability or neurite area were observed after a 24 h MC-LF treatment, we investigated the effects after a longer treatment period. After 48 h MC-LF treatment with 10 µM, a reduction in cell count was observed (Fig. 3C). This was even more pronounced after 48 h of treatment, followed by 48 h of washout (Fig. 3D-F). Under these conditions, not only the cell count was reduced but also the neurites were completely broken down (Fig. 3F). In another approach, we tested whether a 24 h treatment at later time points, namely DoD 4-5, is also sufficient to see a reduction in cell count or neurite area. Therefore, we tested concentrations up to 5 µM MC-LF but we did not observe a reduction in either of the two parameters (Fig. S3E[3]). As alternative toxicity indicator, we considered acute signaling effects as measurable by intracellular calcium changes (Fig. S4A[3]). As positive controls we used cell depolarization by an increase of potassium ions (30 mM) (Fig. S4B[3]) in the medium and exposure to ciguatoxin (15 nM) (Fig. S4C[3]), a polyether marine biotoxin specifically inhibiting voltage-gated Na^+ channels (Daneshian et al., 2013). In both cases, clear increases of intracellular free calcium were observed, while MC-LF (2.5 µM) had no effect at all (Fig. S4A[3]).

4 Conclusions

Both *in vitro* systems used in this study clearly showed, that low µM concentrations of MC lead to human neurotoxicity. Since one of the assays was representative of the peripheral nervous system, which is not protected by a blood-brain barrier, the concentration range identified here would with high likelihood trigger acute human neurotoxicity and may be used as point-of-departure for risk assessment of acute exposure settings. In standard nutritional exposure scenarios (including contaminated drinking water or food), human plasma concentrations are likely to be at least 100-1000 fold below this hazard threshold. It needs to be noted that this risk assessment statement does not account for parenteral exposure. It also does not allow conclusions on lower level exposures occurring over considerably longer times than tested here. A follow-up study on this would require cultures that can be exposed for several weeks, and it may use some of the regulated genes that were identified here as biomarkers of subtle effects.

References

Altaner, S., Puddick, J., Fessard, V. et al. (2019). Simultaneous detection of 14 microcystin congeners from tissue samples using uplc- esi-ms/ms and two different deuterated synthetic microcystins as internal standards. *Toxins 11*, 388. doi:10.3390/toxins11070388

Altaner, S., Jaeger, S., Fotler, R. et al. (2020). Machine learning prediction of cyanobacterial toxin (microcystin) toxicodynamics in humans. *ALTEX 37*, 24-36. doi:10.14573/altex.1904031

Azevedo, S. M. F. O., Carmichael, W. W., Jochimsen, E. M. et al. (2002). Human intoxication by microcystins during renal dialysis treatment in caruaru-brazil. *Toxicology 181-182*, 441-446. doi:10.1016/s0300-483x(02)00491-2

Botes D.P., T. A. A., Wessels P.L., Viljoen C.C., Kruger H., Williams D.H., Santikarn S., Smith R.J. Hammond S.J. (1984). The structure of cyanoginosin-la, a cyclic heptapeptide toxin from the cyanobacterium *microcystis aeruginos*. *J. Chem. Soc. Perkin Trans. I*, 2311-2318.

Bronger, H., König, J., Kopplow, K. et al. (2005). Abcc drug efflux pumps and organic anion uptake transporters in human gliomas and the blood-tumor barrier. *Cancer research 65*, 11419-11428. doi:10.1158/0008-5472.CAN-05-1271

Buratti, F. M., Manganelli, M., Vichi, S. et al. (2017). Cyanotoxins: Producing organisms, occurrence, toxicity, mechanism of action and human health toxicological risk evaluation. *Arch Toxicol 91*, 1049-1130. doi:10.1007/s00204-016-1913-6

Carmichael, W. W. (1992). Cyanobacteria secondary metabolites--the cyanotoxins. *The Journal of applied bacteriology 72*, 445-459. doi:10.1111/j.1365-2672.1992.tb01858.x

Chen, J., Xie, P., Li, L. et al. (2009). First identification of the hepatotoxic microcystins in the serum of a chronically exposed human population together with indication of hepatocellular damage. *Toxicological sciences : an official journal of the Society of Toxicology 108*, 81-89. doi:10.1093/toxsci/kfp009

Chen, L. and Xie, P. (2016). Mechanisms of microcystin-induced cytotoxicity and apoptosis. *Mini Rev Med Chem 16*, 1018-1031. doi:10.2174/1389557516666160219130407

Daneshian, M., Botana, L. M., Dechraoui Bottein, M.-Y. et al. (2013). A roadmap for hazard monitoring and risk assessment of marine biotoxins on the basis of chemical and biological test systems. *ALTEX 30*, 487-545. doi:10.14573/altex.2013.4.487

Delp, J., Gutbier, S., Klima, S. et al. (2018). A high-throughput approach to identify specific neurotoxicants/ developmental toxicants in human neuronal cell function assays. *ALTEX 35*, 235-253. doi:10.14573/altex.1712182

Delp, J., Funke, M., Rudolf, F. et al. (2019). Development of a neurotoxicity assay that is tuned to detect mitochondrial toxicants. *Archives of toxicology 93*, 1585-1608. doi:10.1007/s00204-019-02473-y

Desprez, B., Birk, B., Blaauboer, B. et al. (2019). A mode-of-action ontology model for safety evaluation of chemicals: Outcome of a series of workshops on repeated dose toxicity. *Toxicology in vitro : an international journal published in association with BIBRA 59*, 44-50. doi:10.1016/j.tiv.2019.04.005

Devos, D., Moreau, C., Devedjian, J. C. et al. (2014). Targeting chelatable iron as a therapeutic modality in parkinson's disease. *Antioxidants & redox signaling 21*, 195-210. doi:10.1089/ars.2013.5593

Dietrich, D. and Hoeger, S. (2005). Guidance values for microcystins in water and cyanobacterial supplement products (blue-green algal supplements): A reasonable or misguided approach? *Toxicology and Applied Pharmacology 203*, 273-289. doi:10.1016/j.taap.2004.09.005

Feurstein, D., Holst, K., Fischer, A. et al. (2009). OATP-associated uptake and toxicity of microcystins in primary murine whole brain cells. *Toxicology and applied pharmacology 234*, 247-255. doi:10.1016/j.taap.2008.10.011

Feurstein, D., Stemmer, K., Kleinteich, J. et al. (2011). Microcystin congener- and concentration-dependent induction of murine neuron apoptosis and neurite degeneration. *Toxicological sciences : an official journal of the Society of Toxicology 124*, 424-431. doi:10.1093/toxsci/kfr243

Fischer, W. J. and Dietrich, D. R. (2000). Pathological and biochemical characterization of microcystin-induced hepatopancreas and kidney damage in carp (cyprinus carpio). *Toxicology and applied pharmacology 164*, 73-81. doi:10.1006/taap.1999.8861

Fischer, W. J., Altheimer, S., Cattori, V. et al. (2005). Organic anion transporting polypeptides expressed in liver and brain mediate uptake of microcystin. *Toxicology and applied pharmacology 203*, 257-263. doi:10.1016/j.taap.2004.08.012

Gao, Y.-s., Hubbert, C. C., Lu, J. et al. (2007). Histone deacetylase 6 regulates growth factor-induced actin remodeling and endocytosis. *Molecular and cellular biology 27*, 8637-8647. doi:10.1128/MCB.00393-07

Gutbier, S., Spreng, A.-S., Delp, J. et al. (2018). Prevention of neuronal apoptosis by astrocytes through thiol-mediated stress response modulation and accelerated recovery from proteotoxic stress. *Cell death and differentiation 25*, 2101-2117. doi:10.1038/s41418-018-0229-x

Hagenbuch, B. and Meier, P. J. (2003). The superfamily of organic anion transporting polypeptides. *Biochimica et biophysica acta 1609*, 1-18. doi:10.1016/s0005-2736(02)00633-8

Herrera, N., Herrera, C., Ortíz, I. et al. (2018). Genotoxicity and cytotoxicity of three microcystin-lr containing cyanobacterial samples from antioquia, colombia. *Toxicon : official journal of the International Society on Toxinology 154*, 50-59. doi:10.1016/j.toxicon.2018.09.011

Heussner, A. H., Mazija, L., Fastner, J. et al. (2012). Toxin content and cytotoxicity of algal dietary supplements. *Toxicology and Applied Pharmacology 265*, 263-271. doi:doi:10.1016/j.taap.2012.10.005

Hinojosa, M. G., Gutiérrez-Praena, D., Prieto, A. I. et al. (2019). Neurotoxicity induced by microcystins and cylindrospermopsin: A review. *The Science of the total environment 668*, 547-565. doi:10.1016/j.scitotenv.2019.02.426

Hoelting, L., Klima, S., Karreman, C. et al. (2016). Stem cell-derived immature human dorsal root ganglia neurons to identify peripheral neurotoxicants. *Stem Cells Transl Med 5*, 476-487. doi:10.5966/sctm.2015-0108

Höllerhage, M., Moebius, C., Melms, J. et al. (2017). Protective efficacy of phosphodiesterase-1 inhibition against alpha-synuclein toxicity revealed by compound screening in luhmes cells. *Scientific reports 7*, 11469-11469. doi:10.1038/s41598-017-11664-5

House, J. S., Grimm, F. A., Jima, D. D. et al. (2017). A pipeline for high-throughput concentration response modeling of gene expression for toxicogenomics. *Frontiers in Genetics 8*, doi:10.3389/fgene.2017.00168

Hu, Y., Chen, J., Fan, H. et al. (2016). A review of neurotoxicity of microcystins. *Environmental science and pollution research international 23*, 7211-7219. doi:10.1007/s11356-016-6073-y

Jochimsen, E. M., Carmichael, W. W., An, J. S. et al. (1998). Liver failure and death after exposure to microcystins at a hemodialysis center in brazil. *The New England journal of medicine 338*, 873-878. doi:10.1056/NEJM199803263381304

Karreman, C., Klima, S., Holzer, A. K. et al. (2020). Caffee: A program for evaluating time courses of ca2+ dependent signal changes of complex cells loaded with fluorescent indicator dyes. *Altex 37*, 332-336. doi:10.14573/altex.2003191

Krug, A. K., Balmer, N. V., Matt, F. et al. (2013). Evaluation of a human neurite growth assay as specific screen for developmental neurotoxicants. *Arch Toxicol 87*, 2215-2231. doi:10.1007/s00204-013-1072-y

Li, Y., Chen, J.-a., Zhao, Q. et al. (2011). A cross-sectional investigation of chronic exposure to microcystin in relationship to childhood liver damage in the three gorges reservoir region, china. *Environmental health perspectives 119*, 1483-1488. doi:10.1289/ehp.1002412

Livak, K. J. and Schmittgen, T. D. (2001). Analysis of relative gene expression data using real-time quantitative pcr and the 2(-delta delta c(t)) method. *Methods (San Diego, Calif.) 25*, 402-408. doi:10.1006/meth.2001.1262

Lohren, H., Blagojevic, L., Fitkau, R. et al. (2015). Toxicity of organic and inorganic mercury species in differentiated human neurons and human astrocytes. *Journal of trace elements in medicine and biology : organ of the Society for Minerals and Trace Elements (GMS) 32*, 200-208. doi:10.1016/j.jtemb.2015.06.008

Lotharius, J., Falsig, J., van Beek, J. et al. (2005). Progressive degeneration of human mesencephalic neuron-derived cells triggered by dopamine-dependent oxidative stress is dependent on the mixed-lineage kinase pathway. *The Journal of neuroscience : the official journal of the Society for Neuroscience 25*, 6329-6342. doi:10.1523/JNEUROSCI.1746-05.2005

Love, M. I., Huber, W. and Anders, S. (2014). Moderated estimation of fold change and dispersion for rna-seq data with deseq2. *Genome Biology 15*, 550. doi:10.1186/s13059-014-0550-8

MacKintosh, C., Beattie, K. A., Klumpp, S. et al. (1990). Cyanobacterial microcystin-lr is a potent and specific inhibitor of protein phosphatases 1 and 2a from both mammals and higher plants. *FEBS letters 264*, 187-192. doi:10.1016/0014-5793(90)80245-e

Matelski, L., Morgan, R. K., Grodzki, A. C. et al. (2020). Effects of cytokines on nuclear factor-kappa b, cell viability, and synaptic connectivity in a human neuronal cell line. *Molecular psychiatry* 10.1038/s41380-41020-40647-41382. doi:10.1038/s41380-020-0647-2

Metsalu, T. and Vilo, J. (2015). Clustvis: A web tool for visualizing clustering of multivariate data using principal component analysis and heatmap. *Nucleic Acids Research 43*, W566-W570. doi:10.1093/nar/gkv468

Nishiwaki-Matsushima, R., Ohta, T., Nishiwaki, S. et al. (1992). Liver tumor promotion by the cyanobacterial cyclic peptide toxin microcystin-lr. *Journal of cancer research and clinical oncology 118*, 420-424. doi:10.1007/bf01629424

Pouria, S., de Andrade, A., Barbosa, J. et al. (1998). Fatal microcystin intoxication in haemodialysis unit in caruaru, brazil. *Lancet (London, England) 352*, 21-26. doi:10.1016/s0140-6736(97)12285-1

Raudvere, U., Kolberg, L., Kuzmin, I. et al. (2019). G:Profiler: A web server for functional enrichment analysis and conversions of gene lists (2019 update). *Nucleic Acids Research 47*, W191-W198. doi:10.1093/nar/gkz369

Scholz, D., Pöltl, D., Genewsky, A. et al. (2011). Rapid, complete and large-scale generation of post-mitotic neurons from the human luhmes cell line. *Journal of neurochemistry 119*, 957-971. doi:10.1111/j.1471-4159.2011.07255.x

Scholz, D., Chernyshova, Y., Ückert, A.-K. et al. (2018). Reduced aβ secretion by human neurons under conditions of strongly increased bace activity. *Journal of neurochemistry 147*, 256-274. doi:10.1111/jnc.14467

Singh, N., Lawana, V., Luo, J. et al. (2018). Organophosphate pesticide chlorpyrifos impairs stat1 signaling to induce dopaminergic neurotoxicity: Implications for mitochondria mediated oxidative stress signaling events. *Neurobiology of disease 117*, 82-113. doi:10.1016/j.nbd.2018.05.019

Skirzewski, M., Karavanova, I., Shamir, A. et al. (2018). Erbb4 signaling in dopaminergic axonal projections increases extracellular dopamine levels and regulates spatial/working memory behaviors. *Molecular psychiatry 23*, 2227-2237. doi:10.1038/mp.2017.132

Spoof, L. and Catherine, A. (2016). *Appendix 3: Tables of microcystins and nodularins*. Handbook of cyanobacterial monitoring and cyanotoxin analysis. Vol. doi:10.1002/9781119068761.app3

Stiegler, N. V., Krug, A. K., Matt, F. et al. (2011). Assessment of chemical-induced impairment of human neurite outgrowth by multiparametric live cell imaging in high-density cultures. *Toxicol Sci 121*, 73-87. doi:10.1093/toxsci/kfr034

Svirčev, Z., Lalić, D., Bojadžija Savić, G. et al. (2019). Global geographical and historical overview of cyanotoxin distribution and cyanobacterial poisonings. *Archives of toxicology 93*, 2429-2481. doi:10.1007/s00204-019-02524-4

Tong, Z.-B., Huang, R., Wang, Y. et al. (2018). The toxmatrix: Chemo-genomic profiling identifies interactions that reveal mechanisms of toxicity. *Chemical research in toxicology 31*, 127-136. doi:10.1021/acs.chemrestox.7b00290

Valério, E., Vasconcelos, V. and Campos, A. (2016). New insights on the mode of action of microcystins in animal cells - a review. *Mini Rev Med Chem 16*, 1032-1041. doi:10.2174/1389557516666160219130553

Waldmann, T., Rempel, E., Balmer, N. V. et al. (2014). Design principles of concentration-dependent transcriptome deviations in drug-exposed differentiating stem cells. *Chemical research in toxicology 27*, 408-420. doi:10.1021/tx400402j

Weng, M. K., Zimmer, B., Pöltl, D. et al. (2012). Extensive transcriptional regulation of chromatin modifiers during human neurodevelopment. *PloS one 7*, e36708-e36708. doi:10.1371/journal.pone.0036708

Weng, M. K., Natarajan, K., Scholz, D. et al. (2014). Lineage-specific regulation of epigenetic modifier genes in human liver and brain. *PloS one 9*, e102035-e102035. doi:10.1371/journal.pone.0102035

Witt, B., Meyer, S., Ebert, F. et al. (2017). Toxicity of two classes of arsenolipids and their water-soluble metabolites in human differentiated neurons. *Archives of toxicology 91*, 3121-3134. doi:10.1007/s00204-017-1933-x

Yoshizawa, S., Matsushima, R., Watanabe, M. F. et al. (1990). Inhibition of protein phosphatases by microcystins and nodularin associated with hepatotoxicity. *Journal of cancer research and clinical oncology 116*, 609-614. doi:10.1007/bf01637082

Conflict of interest

The authors declare no conflict of interest.

Acknowledgments

This work was supported by the BMBF, INVITE, EFSA, the DK-EPA (MST-667-00205), and the University of Konstanz. It has received funding from the European Union's Horizon 2020 research and innovation programme under grant agreements No. 681002 (EU-ToxRisk) and No. 825759 (ENDpoiNTs), as well as from CHARM (BadenWürttemberg Wassernetzwerk). We are grateful to Viola Singer and Heidrun Leisner for invaluable experimental support.